In Vivo Characterization of 4 ^{68}Ga-Labeled Multimeric RGD Peptides to Image $\alpha_v\beta_3$ Integrin Expression in 2 Human Tumor Xenograft Mouse Models

Daphne Lobeek[1], Gerben M. Franssen[1], Michelle T. Ma[2], Hans-Jürgen Wester[3], Clemens Decristoforo[4], Wim J.G. Oyen[1,5], Otto C. Boerman[1], Samantha Y.A. Terry*[2], and Mark Rijpkema*[1]

[1]Department of Radiology and Nuclear Medicine, Radboud University Medical Center Nijmegen, Nijmegen, The Netherlands; [2]Department of Imaging Chemistry and Biology, King's College London, London, United Kingdom; [3]Pharmazeutische Radiochemie, Technische Universität München, Garching, Germany; [4]Department of Nuclear Medicine, Medical University Innsbruck, Innsbruck, Austria; and [5]Institute of Cancer Research and Royal Marsden NHS Trust, Department of Nuclear Medicine, London, United Kingdom

$\alpha_v\beta_3$ integrins play an important role in angiogenesis and cell migration in cancer and are highly expressed on the activated endothelial cells of newly formed blood vessels. Here, we compare the targeting characteristics of 4 ^{68}Ga-labeled multimeric cyclic arginine-glycine-aspartate (RGD)–based tracers in an $\alpha_v\beta_3$ integrin–expressing tumor model and a tumor model in which $\alpha_v\beta_3$ integrin is expressed solely on the neovasculature. **Methods:** Female BALB/c nude mice were subcutaneously injected with SK-RC-52 ($\alpha_v\beta_3$ integrin–positive) or FaDu ($\alpha_v\beta_3$ integrin–negative) tumor cells. ^{68}Ga-labeled DOTA-$(RGD)_2$, TRAP-$(RGD)_3$, FSC-$(RGD)_3$, or THP-$(RGD)_3$ was intravenously administered to the mice (0.5 nmol per mouse, 10–20 MBq), followed by small-animal PET/CT imaging and ex vivo biodistribution studies 1 h after injection. Nonspecific uptake of the tracers in both models was determined by coinjecting an excess of unlabeled DOTA-$(RGD)_2$ (50 nmol) along with the radiolabeled tracers. **Results:** Imaging and biodistribution data showed specific uptake in the tumors for each tracer in both models. Tumor uptake of ^{68}Ga-FSC-$(RGD)_3$ was significantly higher than that of ^{68}Ga-DOTA-$(RGD)_2$, ^{68}Ga-TRAP-$(RGD)_3$, or ^{68}Ga-THP-$(RGD)_3$ in the SK-RC-52 model but not in the FaDu model, in which ^{68}Ga-FSC-$(RGD)_3$ showed significantly higher tumor uptake than ^{68}Ga-TRAP-$(RGD)_3$. Most importantly, differences were also observed in normal tissues and in tumor-to-blood ratios. **Conclusion:** All tracers showed sufficient targeting of $\alpha_v\beta_3$ integrin expression to allow for tumor detection. Although the highest tumor uptake was found for ^{68}Ga-FSC-$(RGD)_3$ and ^{68}Ga-THP-$(RGD)_3$ in the SK-RC-52 and FaDu models, respectively, selection of the optimal tracer for specific diagnostic applications also depends on tumor-to-blood ratio and uptake in normal tissues; these factors should therefore also be considered.

Key Words: $\alpha_v\beta_3$ integrin; RGD peptides; multimers; angiogenesis; ^{68}Ga

J Nucl Med 2018; 59:1296–1301
DOI: 10.2967/jnumed.117.206979

Molecular imaging of $\alpha_v\beta_3$ integrin expression with SPECT or PET is a promising technique that allows for visualization of tumor angiogenesis. $\alpha_v\beta_3$ integrins are transmembrane proteins recognizing the arginine-glycine-aspartate (RGD) sequence of extracellular matrix proteins. $\alpha_v\beta_3$ integrins are expressed on the cell membrane of several solid tumors, thereby modulating tumor growth and metastasis (*1*). During angiogenesis, activated $\alpha_v\beta_3$ integrins are expressed on the endothelial cells of newly formed vessels, inducing gene-expression and cytoskeleton changes and regulating the growth and survival of tumor cells (*2*). $\alpha_v\beta_3$ integrins are studied as targets for tumor-targeted therapies (*3*), for RGD–drug conjugates (*4*), and for molecular imaging agents to further characterize tumors and predict or assess response to antiangiogenic cancer therapies (*5*).

A series of RGD derivatives for in vivo imaging of $\alpha_v\beta_3$ integrins has been developed using different approaches to obtain ligands with high in vivo stability, high affinity for $\alpha_v\beta_3$ integrins, and optimal pharmacokinetics (*6*). It has been shown that cyclization of linear RGD peptides and multimerization improve the binding affinity of RGD ligands for $\alpha_v\beta_3$ integrins (*7–10*). For wider adoption of PET and SPECT imaging of $\alpha_v\beta_3$ integrin expression in the clinic, radiolabeled ligands require straightforward, robust, and efficient labeling protocols. The most recently developed ligands can be radiolabeled efficiently (>90%) and rapidly (<15 min) with ^{68}Ga—in some cases, at room temperature and under mild conditions (near-neutral pH)—making them suitable for routine clinical radiosynthesis (*7,11–14*). Because of the excellent physical characteristics of ^{68}Ga (short half-life [68 min] and high positron yield [89%]), and the availability of good-manufacturing-practice–compliant ^{68}Ge/^{68}Ga generators, ^{68}Ga-labeled RGD peptides can now be considered as tracers for PET imaging of angiogenesis.

There have been major efforts to develop stable ^{68}Ga-labeled RGD peptides, and several monomeric ^{68}Ga-binding bifunctional chelators have been studied, including ^{68}Ga-NOTA-RGD in lung cancer and lymphoma patients (*15*) and ^{68}Ga-NODAGA-RGD in hepatocellular carcinoma (*16*). However, dimeric, trimeric, and tetrameric RGD analogs have shown higher specific accumulation in $\alpha_v\beta_3$ integrin–expressing tumors than have their monomeric counterparts (*7–10*). Four recently developed multimeric ^{68}Ga-labeled RGD peptides with good in vivo imaging characteristics

Received Dec. 15, 2017; revision accepted Feb. 12, 2018.
For correspondence or reprints contact: Daphne Lobeek, Department of Radiology and Nuclear Medicine, Radboud University Medical Center, P.O. Box 9101, 6500 HB, Nijmegen, Netherlands.
E-mail: daphne.lobeek@radboudumc.nl
*Contributed equally to this work.
Published online Apr. 6, 2018.

are ^{68}Ga-DOTA-(RGD)$_2$ (1,4,7,10-tetraazacyclododecane-1,4,7,10-tetraacetic acid) (*7,8*), ^{68}Ga-TRAP-(RGD)$_3$ (1,4,7-triazacyclononane-1,4,7-tris[(2-carboxyethyl)methylenephosphinic acid]) (*11,17*), ^{68}Ga-FSC-(RGD)$_3$ (fusarinine-C) (*12,18*), and ^{68}Ga-THP-(RGD)$_3$ (tris(hydroxypyridinone)) (*13,19*). These peptides are based on different chelators, each with different topologic arrangements of multimeric cyclic-RGDfK peptides (Fig. 1). At physiologic pH, all of these ^{68}Ga-chelator motifs are neutrally charged. These 4 $\alpha_v\beta_3$ integrin–targeted tracers have been assessed preclinically in vitro, in vivo, and ex vivo (*8,11,12,17–19*), but in separate experiments using different murine tumor models with high levels of $\alpha_v\beta_3$ integrin expression. To directly compare their imaging characteristics, we assessed their in vivo and ex vivo behavior under standardized conditions and in the same experimental set-up, an $\alpha_v\beta_3$ integrin–positive human xenograft tumor model (SK-RC-52). Furthermore, to assess their potential to image angiogenesis, we also compared their targeting characteristics in an $\alpha_v\beta_3$ integrin–negative tumor model (FaDu, which expresses $\alpha_v\beta_3$ integrin only on the neovasculature).

MATERIALS AND METHODS

Synthesis and Radiolabeling of RGD Peptides

DOTA-(RGD)$_2$ (molecular weight, 1,704.8 g/mol), TRAP-(RGD)$_3$ (3,145.0 g/mol), FSC-(RGD)$_3$ (2,782.3 g/mol), and THP-(RGD)$_3$ (3,720.6 g/mol) were synthesized as described previously (*7,8,11,12,17–19*). Their structures are shown in Figure 1. They were labeled with ^{68}Ga eluted with 0.1 M HCl from an IGG101 TiO_2-based ^{68}Ge/^{68}Ga generator (GalliaPharm; Eckert and Ziegler). Three fractions of 0.5–1 mL were collected, and the second fraction (that with the highest activity) was used to label the peptides.

^{68}Ga-labeled DOTA-(RGD)$_2$ (6 μg) and TRAP-(RGD)$_3$ (11 μg) were prepared by mixing the RGD peptide (1 μg/μL), ^{68}Ga (700 μL, 142–168 MBq), and 4-(2-hydroxyethyl)-1-piperazineethanesulfonic acid buffer (2.5 M, 88 μL) for 20 min (DOTA-(RGD)$_2$) or 5 min (TRAP-(RGD)$_3$) at 95°C. ^{68}Ga-labeled FSC-(RGD)$_3$ (10 μg) and THP-(RGD)$_3$ (13 μg) were prepared by mixing the RGD peptide (1 μg/μL), ^{68}Ga-eluate (700 μL, 105–196 MBq), and aqueous sodium acetate solution (150 μL 0.5 M), in an Eppendorf LoBind protein tube for 15 min at room temperature.

All tracers were further diluted (10–20 MBq in 0.3 mL) in phosphate-buffered saline (0.1 M, pH 7.4) with 0.5% bovine serum albumin for in vivo studies.

Quality Control

Instant thin-layer chromatography analysis of all ^{68}Ga-labeled RGD peptides was performed with Varian silica gel strips (Agilent Technologies), using 0.1 M (pH 5.5) citrate as the mobile phase for ^{68}Ga-FSC-(RGD)$_3$ and an aqueous solution containing ammonium acetate (0.1 M) and ethylenediamine tetraacetic acid (0.1 M, pH 5.5) (1:1 v/v) as the mobile phase for ^{68}Ga-DOTA-(RGD)$_2$, ^{68}Ga-TRAP-(RGD)$_3$, and ^{68}Ga-THP-(RGD)$_3$. The strips were analyzed using a Fujifilm BAS-1800II scanner (Fuji Photo Film Co.) and Aida software (version 4.21; Raytest GmbH).

The radiochemical purities were also determined by reverse-phase high-performance liquid chromatography on an Agilent 1200 system (Agilent Technologies) using a C18 column (RX-C18, 4.6 × 250 mm; Zorbax) eluted with a gradient mobile phase (0–5 min, 97% solvent A; 5–15 min, 97% solvent A to 0% solvent A [solvent A = 0.1% trifluoroacetic acid in H_2O, solvent B = 0.1% trifluoroacetic acid in acetonitrile]) at 1 mL/min. The radioactivity of the eluate was monitored using an in-line NaI radiodetector. Elution profiles were analyzed using Gina Star software (version 5.9; Raytest GmbH).

Solid-Phase $\alpha_v\beta_3$ Integrin–Binding Assay

The half-maximal inhibitory concentration (IC_{50}) of DOTA-(RGD)$_2$, TRAP-(RGD)$_3$, FSC-(RGD)$_3$, and THP-(RGD)$_3$ for binding $\alpha_v\beta_3$ integrin was determined using a solid-phase competitive binding assay, with ^{111}In-labeled DOTA-(RGD)$_2$ as the readout tracer. The binding assays were performed as described previously (*8*). ^{111}In-labeled DOTA-(RGD)$_2$ was prepared by adding 29.9 μL (16 MBq) of $^{111}InCl_3$ solution to 1 μg of peptide dissolved in 60 μL of 0.5 M 2-(*N*-morpholino)ethanesulfonic acid buffer, pH 5.5, and was further purified on an Oasis HLB (1 cm^3, 30 mg) cartridge (Waters). Radiochemical purity was determined by instant thin-layer chromatography, as described for the ^{68}Ga-labeled tracer.

Two 96-well vinyl microtiter plates (Corning B.V.) were coated with a solution of purified human $\alpha_v\beta_3$ integrin (150 ng/mL, 100 μL/well) (Chemicon International) in coating buffer (25 mM Tris-HCl, pH 7.4, 150 mM NaCl, 1 mM $CaCl_2$, 0.5 mM $MgCl_2$, and 1 mM $MnCl_2$). Nonspecific binding was assessed by blocking with 1% bovine serum albumin in coating buffer (200 μL/well). The appropriate peptide dilution (3 μM to 5×10^{-5} μM, 50 μL/well) and ^{111}In-DOTA-(RGD)$_2$ (50 μL/well) were added. After incubation, the wells were washed and cut out of the plates. The amount of radioactivity in each well was determined using a γ-counter (PerkinElmer Inc.). For each tracer, triplicate measurements were performed.

Cell Lines and Animal Studies

The in vivo behavior of ^{68}Ga-DOTA-(RGD)$_2$, ^{68}Ga-TRAP-(RGD)$_3$, ^{68}Ga-FSC-(RGD)$_3$, and ^{68}Ga-THP-(RGD)$_3$ was determined in 2 different tumor models in mice. The first model had subcutaneous SK-RC-52 human renal cell carcinoma xenografts (tumor cells expressing $\alpha_v\beta_3$ integrins on both tumor cell membrane and neovasculature; $\alpha_v\beta_3$ integrin–positive tumors), and the second, which was used to study RGD uptake in the tumor neovasculature only, had subcutaneous FaDu human squamous cell carcinoma xenografts (tumor cells expressing $\alpha_v\beta_3$ integrin solely on the neovasculature; $\alpha_v\beta_3$ integrin–negative tumors (*21*)). Both tumor cell lines were obtained from the American Type Culture Collection and cultured in RPMI 1640 medium (Gibco, BRL Life Sciences Technologies), supplemented with 1% glutamine (Gibco) and 10% fetal calf serum (Sigma-Aldrich Chemie BV) (RPMI+) at 37°C in a humidified atmosphere with 5% CO_2. Before subcutaneous inoculation, the tumor cells were washed in phosphate-buffered saline, harvested with 0.25% trypsin (5 min at 37°C in a humidified atmosphere with 5% CO_2), counted, spun down (5 min at 1,000*g*), and resuspended to the appropriate concentration with RPMI+. The mice were injected subcutaneously in the left flank with SK-RC-52 cells (2×10^6 cells in 0.2 mL of RPMI+ per mouse) or FaDu cells (4.5×10^6 cells in 0.2 mL of RPMI+ per mouse). Tumors were allowed to grow until they reached a volume of approximately 200 mm^3 as determined by caliper measurements in 3 dimensions.

The animal studies were approved by the Animal Welfare Body of the Radboud University Medical Center Nijmegen and were performed in accordance with the Dutch legislation (Dutch Act on Animal Experimentation). Sixty-four female athymic BALB/c AnNRj-*Foxn1$^{nu/nu}$* nude mice (6–8 wk old; Janvier Labs) were acclimatized for 7 d after transportation to the animal facility. They were housed in filter-topped cages (3 or 5 mice per cage) in a specific pathogen-free unit under standard laboratory conditions (day–night rhythm, 12 h–12 h; room temperature, 20°C–24°C; relative humidity, 50%–60%) and had free access to water and animal chow (Ssniff Spezialdiäten GmbH).

Biodistribution Studies and Small-Animal PET/CT Imaging

Mice with SK-RC-52 (4 groups, 5 mice per group) or FaDu (4 groups, 5 mice per group) tumors were intravenously injected with ^{68}Ga-DOTA-(RGD)$_2$, ^{68}Ga-TRAP-(RGD)$_3$, ^{68}Ga-FSC-(RGD)$_3$, or ^{68}Ga-THP-(RGD)$_3$ (0.5 nmol, 10–20 MBq in 0.3 mL) via the tail vein while awake. The mice were warmed with a heat lamp for

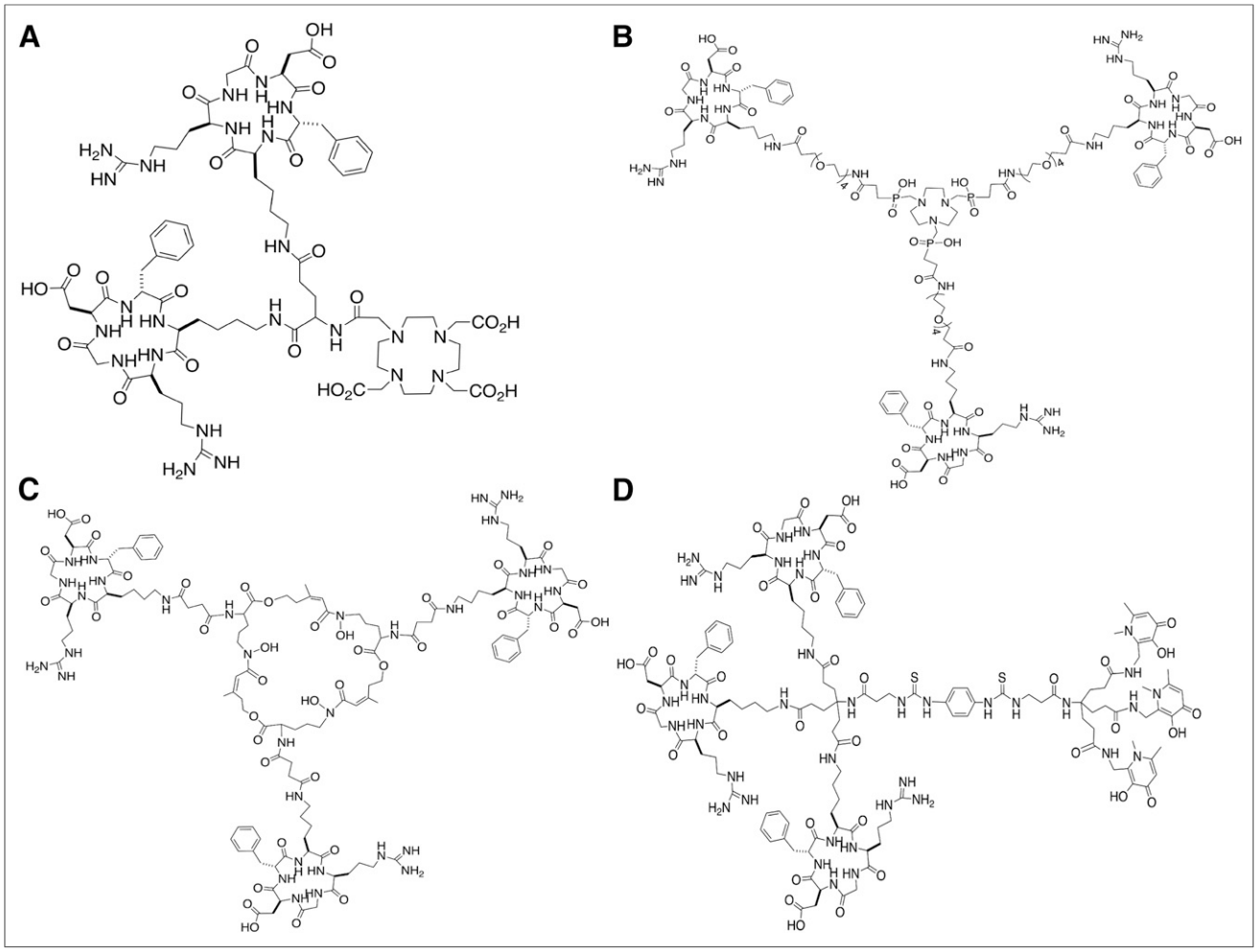

FIGURE 1. Structures of unlabeled DOTA-$(RGD)_2$ (A), TRAP-$(RGD)_3$ (B), FSC-$(RGD)_3$ (C), and THP-$(RGD)_3$ (D).

several minutes before injection. To study the non–$\alpha_v\beta_3$ integrin-mediated localization of the 4 peptides, separate groups of mice (8 groups, 3 mice per group) were coinjected with a 50-nmol (86 μg) excess of unlabeled DOTA-$(RGD)_2$.

All mice were euthanized by CO_2/O_2 asphyxiation 1 h after injection, and tissue samples were dissected and weighed. Additionally, the salivary glands of mice bearing FaDu tumors were dissected and weighed. Uptake of the radiolabeled peptides was calculated as percentage injected dose per gram of tissue (%ID/g), as determined by the γ-counter while simultaneously measuring 1% standards.

Small-animal PET/CT scans were obtained directly after euthanasia (2–3 mice per group). The mice were positioned supine in the scanner (Inveon; Siemens Preclinical Solutions), which had an intrinsic spatial resolution of 1.5 mm, and were consecutively scanned for 20, 30, or 40 min to acquire PET data. For anatomic localization, a CT scan was acquired directly after the PET acquisition, with a spatial resolution of 113 μm (80 kV and 500 μA, with an exposure time of 300 ms).

PET data were reconstructed using Inveon Acquisition Workplace software, version 2.04 (Siemens Preclinical Solutions), with an ordered-subset expectation maximization 3-dimensional maximum a posteriori algorithm, a matrix of 256 × 256 × 161, a pixel size of 0.40 × 0.40 × 0.796 mm, 16 subsets, and 2 iterations. Postreconstruction filtering was applied using a 3-dimensional gaussian filter kernel of 1.5 mm in full width at half maximum. CT data were reconstructed using the same software, with a modified Feldkamp algorithm. The resulting matrix was 768 × 786 pixels with 512 transverse slices (voxel size, 110.5 × 110.5 × 110.5 μm). PET and CT images were fused for anatomic reference using automatic rigid registration software available at the workstation. Before image interpretation, the registration was visually checked.

Statistical Analysis

The IC_{50} values for the radiolabeled peptides were calculated using a nonlinear regression model in GraphPad Prism, version 5.03 (GraphPad Software), and the derived IC_{50} values were compared using a 1-way ANOVA corrected for multiple comparisons by Bonferroni adjustment. Data from the biodistribution studies were expressed as mean %ID/g ± SD. Differences in tumor, blood, and salivary gland (as an example of relevant normal tissue) uptake among the 4 peptides were determined using SPSS Statistics, version 22.0.0.1 (IBM), with a 1-way ANOVA followed by a Bonferroni post hoc test to adjust for multiple comparisons. The level of significance was set to a P value of less than 0.05.

RESULTS

Radiolabeling

Labeling efficiency exceeded 95% for all 4 compounds, as determined with instant thin-layer chromatography and high-performance liquid chromatography. Mean molar activities directly after radiolabeling were 49.1 MBq/nmol for ^{68}Ga-DOTA-$(RGD)_2$, 42.3 MBq/nmol for ^{68}Ga-TRAP-$(RGD)_3$, 55.2 MBq/nmol for ^{68}Ga-FSC-$(RGD)_3$, and 42.6 MBq/nmol for ^{68}Ga-THP-$(RGD)_3$. Retention

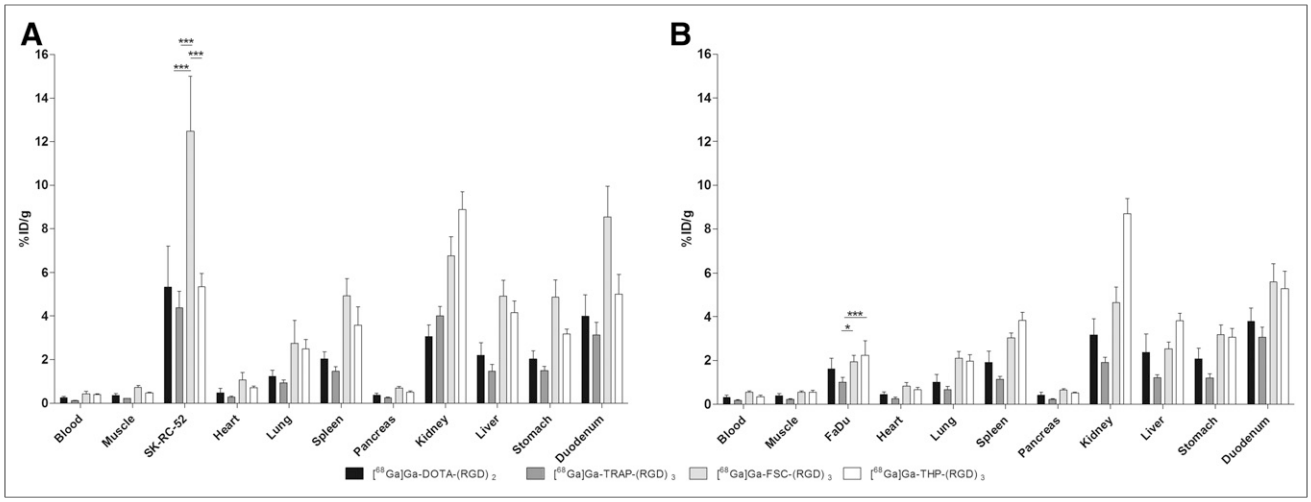

FIGURE 2. Biodistribution of ^{68}Ga-labeled RGD peptides in mice with SK-RC-52 (A) or FaDu (B) tumors. Tissues and organs were dissected 1 h after injection. Data are mean ± SD. *$P < 0.05$. ***$P < 0.001$.

times in the high-performance liquid chromatography elution profiles ranged from 11.9 to 14.9 min.

Competitive Binding Assay

The IC_{50} values of DOTA-$(RGD)_2$, TRAP-$(RGD)_3$, FSC-$(RGD)_3$, and THP-$(RGD)_3$ for $\alpha_v\beta_3$ integrin were determined in a competitive binding assay. Binding of ^{111}In-labeled DOTA-$(RGD)_2$ to $\alpha_v\beta_3$ integrin was determined in the presence of increasing concentrations of unlabeled peptide (Supplemental Fig. 1; supplemental materials are available at http://jnm.snmjournals.org). IC_{50} significantly differed among the 4 peptides ($F_{3,8} = 13.4$, $P = 0.002$). The IC_{50} of dimeric DOTA-$(RGD)_2$ (3.8 ± 0.7 nM) was significantly lower than that of the trimeric TRAP-$(RGD)_3$ (10.0 ± 1.8 nM, $P = 0.005$), FSC-$(RGD)_3$, (9.0 ± 1.6 nM, $P = 0.006$), and THP-$(RGD)_3$ (11.4 ± 1.9 nM, $P = 0.003$). IC_{50} did not significantly differ among the 3 trimeric peptides ($P = 0.7$).

Biodistribution Studies

The biodistribution 1 h after injection of the ^{68}Ga-labeled peptides is presented in Figure 2. The experiments were performed in 2 sessions within 4 consecutive days.

In the SK-RC-52 model, mean tumor uptake of ^{68}Ga-FSC-$(RGD)_3$ (12.5 ± 2.5 %ID/g) was significantly higher than that of ^{68}Ga-DOTA-$(RGD)_2$ (5.3 ± 1.9 %ID/g, $P < 0.0005$), ^{68}Ga-TRAP-$(RGD)_3$ (4.4 ± 0.8 %ID/g, $P < 0.0005$), and ^{68}Ga-THP-$(RGD)_3$ (5.3 ± 0.6 %ID/g, $P < 0.0005$). In the FaDu model, mean tumor uptake of ^{68}Ga-FSC-$(RGD)_3$ (1.9 ± 0.3 %ID/g) was significantly higher than that of ^{68}Ga-TRAP-$(RGD)_3$ (1.0 ± 0.2 %ID/g, $P = 0.026$) but did not significantly differ from that of ^{68}Ga-DOTA-$(RGD)_2$ (1.6 ± 0.5 %ID/g, $P = 1.0$) or ^{68}Ga-THP-$(RGD)_3$ (2.2 ± 0.7 %ID/g, $P = 1.0$). In this model, there was also a significant difference in tumor uptake between ^{68}Ga-TRAP-$(RGD)_3$ and ^{68}Ga-THP-$(RGD)_3$ ($P = 0.002$).

Coinjection of an excess of unlabeled DOTA-$(RGD)_2$ with the radiolabeled RGD peptides significantly reduced tracer uptake in both the SK-RC-52 tumors and the FaDu tumors, demonstrating the receptor-specific uptake of each of the 4 radiolabeled peptides (Supplemental Figs. 2 and 3). The tumor-to-blood ratios for ^{68}Ga-DOTA-$(RGD)_2$, ^{68}Ga-TRAP-$(RGD)_3$, ^{68}Ga-FSC-$(RGD)_3$, and ^{68}Ga-THP-$(RGD)_3$ in the SK-RC-52 model were 24.4 ± 16.0, 38.5 ± 3.8, 30.7 ± 8.1, and 13.5 ± 1.5, respectively, which are

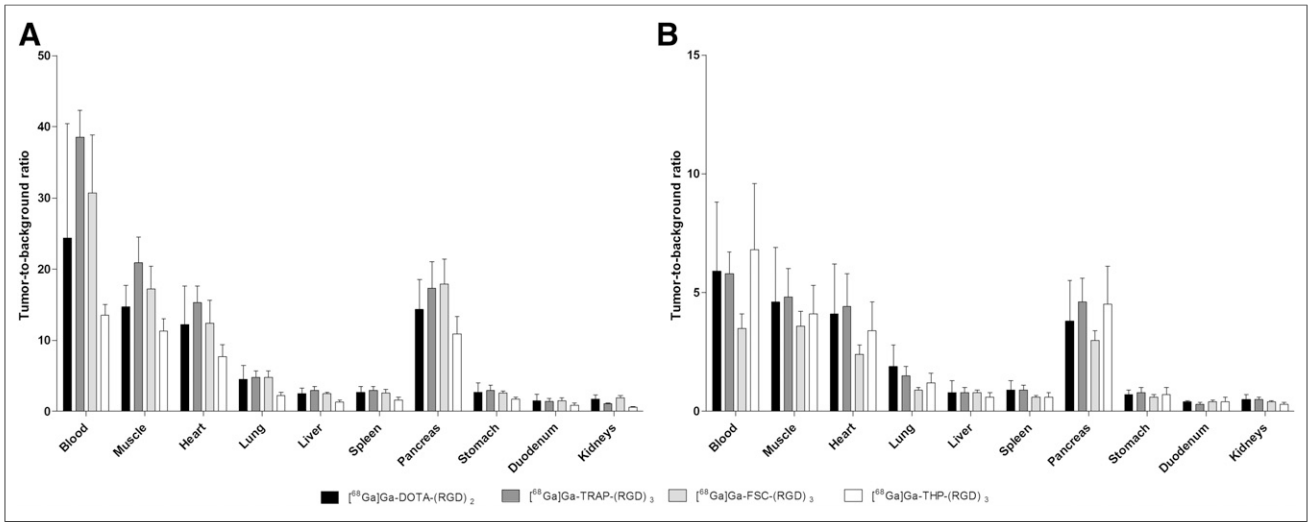

FIGURE 3. Tumor-to-background ratios of ^{68}Ga-labeled RGD peptides in mice with SK-RC-52 (A) or FaDu (B) tumors.

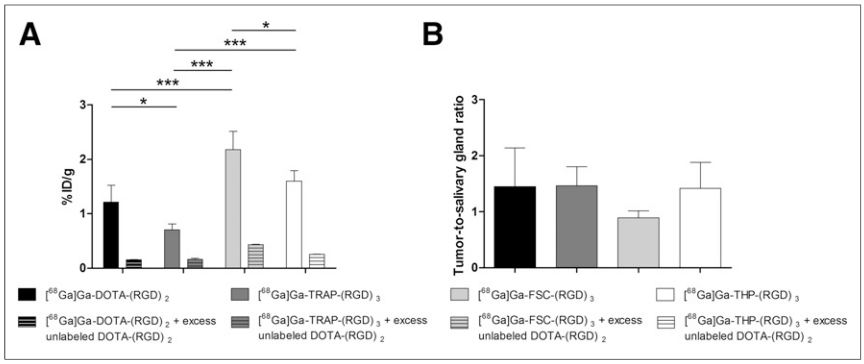

FIGURE 4. Uptake of ^{68}Ga-labeled RGD peptides in salivary glands (A) and tumor–to–salivary gland ratio (B) in mice with FaDu tumors. Data are mean ± SD. $^{*}P < 0.05$. $^{***}P < 0.005$.

markedly higher than in the FaDu model (5.9 ± 2.9, 5.8 ± 0.9, 3.5 ± 0.6, and 6.8 ± 2.8, respectively). In the SK-RC-52 model, the tumor-to-blood ratio significantly differed between ^{68}Ga-TRAP-(RGD)$_3$ and ^{68}Ga-THP-(RGD)$_3$ ($P = 0.012$). No statistically significant differences in tumor-to-blood ratios were observed among the other RGD peptides ($P > 0.05$). Although individual differences in SK-RC-52 tumor-to-tissue ratios were observed among the 4 peptides, no such differences were observed for the FaDu tumor-to-tissue ratios (Fig. 3; Supplemental Table 1). Tracer uptake in salivary glands, as an example of a relevant normal tissue, differed significantly among ^{68}Ga-DOTA-(RGD)$_2$ (1.2 ± 0.3 %ID/g), ^{68}Ga-TRAP-(RGD)$_3$ (0.7 ± 0.1 %ID/g), ^{68}Ga-FSC-(RGD)$_3$ (2.2 ± 0.3 %ID/g), and ^{68}Ga-THP-(RGD)$_3$ (1.6 ± 0.2 %ID/g) in the FaDu model (Fig. 4).

Small-Animal PET/CT Images

Findings on the PET/CT images were in line with the biodistribution data. The SK-RC-52 tumors were clearly visualized, but high uptake was also seen in the kidneys and intestines (Fig. 5). In the FaDu tumors, uptake of all 4 tracers was visible despite high uptake in normal tissues; the signal intensities were in line with the biodistribution studies (Supplemental Fig. 4).

DISCUSSION

This study systematically compared the in vivo targeting characteristics of 1 dimeric and 3 trimeric ^{68}Ga-labeled RGD peptides. All showed receptor-specific uptake and were able to image integrin expression not only in an $\alpha_v\beta_3$ integrin–positive model (Fig. 5) but also in a model expressing $\alpha_v\beta_3$ integrins only on the tumor neovasculature (Supplemental Fig. 4), thus demonstrating potential for imaging low-level integrin expression.

Various strategies have been considered to develop RGD-based peptides with optimal imaging characteristics. Previously reported experiments with multimeric RGD peptides, including ^{68}Ga-DOTA-(RGD)$_2$, ^{68}Ga-TRAP-(RGD)$_3$, ^{68}Ga-FSC-(RGD)$_3$, and ^{68}Ga-THP-(RGD)$_3$, showed improved tumor targeting compared with monomeric RGD peptides (*8,17–19*). In our head-to-head comparison, differences in both absolute tumor uptake and tumor–to–normal-tissue ratios were observed among multimeric compounds. Absolute tumor uptake was highest for ^{68}Ga-FSC-(RGD)$_3$ in SK-RC-52 tumors and for ^{68}Ga-THP-(RGD)$_3$ in FaDu tumors. However, this enhanced uptake of ^{68}Ga-FSC-(RGD)$_3$ and ^{68}Ga-THP-(RGD)$_3$ in the tumors did not improve imaging quality in terms of enhanced tumor–to–normal-tissue ratios (Fig. 3). Concomitant tracer accumulation in nontarget organs such as the spleen, kidneys, liver, and duodenum was shown to be $\alpha_v\beta_3$ integrin–mediated (Supplemental Fig. 2), presumably because of $\alpha_v\beta_3$ integrin expression on the endothelial cells in these organs (*20–22*). These findings are in line with previously published data (*8,23*).

Whereas in vivo studies with RGD peptides focus mainly on high affinities for $\alpha_v\beta_3$ integrin, fast blood clearance, and in vivo stability, successful clinical translation is essentially dependent on high-contrast images with low uptake in nontarget organs. The optimal imaging time point to achieve this goal may be different for the different RGD tracers (*17,18*). In the current study, we assessed only the in vivo behavior of ^{68}Ga-labeled RGD peptides at 60 min after injection. Enhanced tracer accumulation in background organs such as the liver and spleen may hamper the assessment of metastatic spread (*24*). Furthermore, adequate interpretation of PET images and quantification of tracer uptake in the neovasculature may suffer from high $\alpha_v\beta_3$ integrin–mediated uptake in nontumor tissues. For example, in patients with head and neck cancer, uptake in the salivary glands may interfere with visualization of angiogenesis in tumors (Fig. 4). Uptake in the salivary glands was 2-fold higher for ^{68}Ga-FSC-(RGD)$_3$ and ^{68}Ga-THP-(RGD)$_3$ than for ^{68}Ga-DOTA-(RGD)$_2$ and ^{68}Ga-TRAP-(RGD)$_3$. Thus, uptake in background tissues is a relevant consideration in selecting the optimal RGD-based tracer for imaging $\alpha_v\beta_3$ integrin–expressing tumors (Fig. 3). However, Beer et al., in their ^{18}F-galacto-RGD PET/CT study on patients with squamous cell carcinoma of the head and neck, showed that despite uptake in the salivary glands, the images could be interpreted adequately and tumor uptake could be measured accurately (*25*).

In the current study, the in vivo tracer behavior differed between the 2 models: a significantly higher tumor accumulation in mice with SK-RC-52 tumors was found for ^{68}Ga-FSC-(RGD)$_3$, whereas in the FaDu model only significantly lower uptake for ^{68}Ga-TRAP-(RGD)$_3$ was observed. The reasons leading to these differences are unknown. It has been hypothesized that the enhanced tumor uptake of multimeric RGD tracers is due to simultaneous binding of more than 1 RGD unit to $\alpha_v\beta_3$ integrins. However, this possibility is unlikely given the limited spacer length between the RGD units (*26,27*). It is possible that the different levels of

FIGURE 5. Typical PET/CT images of mice with SK-RC-52 tumors (arrows).

$\alpha_v\beta_3$ integrin expression in the 2 models result in differences in relative tumor uptake among ^{68}Ga-labeled radiotracers. At the higher $\alpha_v\beta_3$ expression levels in the SK-RC-52 model, affinity enhancement due to statistical rebinding of multimeric RGD tracers might play a more important role (*28*). In addition, the pharmacokinetic behavior of the ^{68}Ga-labeled tracers will be influenced by the topology and structural arrangement of the conjugated RGD peptides (e.g., distance between RGD units), as well as by differences between the ^{68}Ga-chelator complexes themselves (e.g., lipophilicity and molecular structure).

Molecular imaging of $\alpha_v\beta_3$ integrin expression with radiolabeled RGD peptides has been studied in several clinical applications. RGD PET/CT has allowed imaging of tumors and their metastases and has provided supporting diagnostic information on tumor angiogenesis complementary to that from ^{18}F-FDG PET/CT (*29–32*). Radiolabeled RGD analogs have also been studied as tools to monitor therapy response, both preclinically (*5*) and clinically (*32–34*). The use of ^{68}Ga as a radionuclide for imaging offers the advantages of high sensitivity and resolution combined with onsite availability from generators. In addition, ^{68}Ga-FSC-$(RGD)_3$ can also be labeled with ^{89}Zr, and DOTA-$(RGD)_2$ can also be used with a wide variety of other trivalent radiometals, including ^{111}In for SPECT imaging.

CONCLUSION

This study found that in vivo targeting characteristics differ among ^{68}Ga-DOTA-$(RGD)_2$, ^{68}Ga-TRAP-$(RGD)_3$, ^{68}Ga-FSC-$(RGD)_3$, and ^{68}Ga-THP-$(RGD)_3$. Although most of these differences were not statistically significant, tumor uptake in the SK-RC-52 and FaDu models was highest for ^{68}Ga-FSC-$(RGD)_3$ and ^{68}Ga-THP-$(RGD)_3$, respectively. With consideration of binding affinity, radiolabeling properties, and uptake in both tumor and normal tissues, the most suitable radiolabeled RGD peptide for a specific diagnostic application can be selected.

DISCLOSURE

This work was supported by King's College London and UCL Comprehensive Cancer Imaging Centre, funded by the CRUK and EPSRC in association with the MRC and DoH (England) and by the Wellcome/EPSRC Centre for Medical Engineering (WT 203148/Z/16/Z). No other potential conflict of interest relevant to this article was reported.

ACKNOWLEDGMENTS

We thank Iris Lamers-Elemans, Kitty Lemmens-Hermans, Bianca Lemmers-van de Weem, and Maikel School of the animal facility for technical assistance during the experiments.

REFERENCES

1. Brakebusch C, Bouvard D, Stanchi F, Sakai T, Fassler R. Integrins in invasive growth. *J Clin Invest.* 2002;109:999–1006.
2. Hood JD, Cheresh DA. Role of integrins in cell invasion and migration. *Nat Rev Cancer.* 2002;2:91–100.
3. Katsamakas S, Chatzisideri T, Thysiadis S, Sarli V. RGD-mediated delivery of small-molecule drugs. *Future Med Chem.* 2017;9:579–604.
4. Dal Corso A, Pignataro L, Belvisi L, Gennari C. αvβ3 integrin-targeted peptide/peptidomimetic-drug conjugates: in-depth analysis of the linker technology. *Curr Top Med Chem.* 2016;16:314–329.
5. Terry SY, Abiraj K, Lok J, et al. Can ^{111}In-RGD2 monitor response to therapy in head and neck tumor xenografts? *J Nucl Med.* 2014;55:1849–1855.
6. Haubner R, Maschauer S, Prante O. PET radiopharmaceuticals for imaging integrin expression: tracers in clinical studies and recent developments. *Biomed Res Int.* 2014;2014:871609.
7. Dijkgraaf I, Kruijtzer JA, Liu S, et al. Improved targeting of the $\alpha_v\beta_3$ integrin by multimerisation of RGD peptides. *Eur J Nucl Med Mol Imaging.* 2007;34:267–273.
8. Dijkgraaf I, Yim CB, Franssen GM, et al. PET imaging of $\alpha_v\beta_3$ integrin expression in tumours with ^{68}Ga-labelled mono-, di- and tetrameric RGD peptides. *Eur J Nucl Med Mol Imaging.* 2011;38:128–137.
9. Poethko T, Thumshirn G, Hersel U, et al. Improved tumor uptake, tumor retention and tumor/background ratios of pegylated RGD-multimers [abstract]. *J Nucl Med.* 2003;44(suppl):46p.
10. Thumshirn G, Hersel U, Goodman SL, Kessler H. Multimeric cyclic RGD peptides as potential tools for tumor targeting: solid-phase peptide synthesis and chemoselective oxime ligation. *Chemistry.* 2003;9:2717–2725.
11. Notni J, Simecek J, Hermann P, Wester HJ. TRAP, a powerful and versatile framework for gallium-68 radiopharmaceuticals. *Chemistry.* 2011;17:14718–14722.
12. Knetsch PA, Zhai C, Rangger C, et al. [^{68}Ga]FSC-$(RGD)_3$ a trimeric RGD peptide for imaging alphavbeta3 integrin expression based on a novel siderophore derived chelating scaffold-synthesis and evaluation. *Nucl Med Biol.* 2015;42:115–122.
13. Ma MT, Cullinane C, Imberti C, et al. New tris(hydroxypyridinone) bifunctional chelators containing isothiocyanate groups provide a versatile platform for rapid one step labeling and PET imaging with Ga-68(3+). *Bioconjug Chem.* 2016;27:309–318.
14. Ma MT, Cullinane C, Waldeck K, Roselt P, Hicks RJ, Blower PJ. Rapid kit-based ^{68}Ga-labelling and PET imaging with THP-Tyr_3-octreotate: a preliminary comparison with DOTA-Tyr_3-octreotate. *EJNMMI Res.* 2015;5:52.
15. Kim JH, Lee JS, Kang KW, et al. Whole-body distribution and radiation dosimetry of ^{68}Ga-NOTA-RGD, a positron emission tomography agent for angiogenesis imaging. *Cancer Biother Radiopharm.* 2012;27:65–71.
16. Haubner R, Finkenstedt A, Stegmayr A, et al. [^{68}Ga]NODAGA-RGD: metabolic stability, biodistribution, and dosimetry data from patients with hepatocellular carcinoma and liver cirrhosis. *Eur J Nucl Med Mol Imaging.* 2016;43:2005–2013.
17. Notni J, Pohle K, Wester HJ. Be spoilt for choice with radiolabelled RGD peptides: preclinical evaluation of ^{68}Ga-TRAP$(RGD)_3$. *Nucl Med Biol.* 2013;40:33–41.
18. Zhai C, Franssen GM, Petrik M, et al. Comparison of Ga-68-labeled fusarinine C-based multivalent RGD conjugates and [Ga]NODAGA-RGD: in vivo imaging studies in human xenograft tumors. *Mol Imaging Biol.* 2016;18:758–767.
19. Imberti C, Terry SY, Cullinane C, et al. Enhancing PET signal at target tissue in vivo: dendritic and multimeric tris(hydroxypyridinone) conjugates for molecular imaging of alphavbeta3 integrin expression with gallium-68. *Bioconjug Chem.* 2017;28:481–495.
20. Terry SY, Abiraj K, Frielink C, et al. Imaging integrin $\alpha_v\beta_3$ on blood vessels with ^{111}In-RGD_2 in head and neck tumor xenografts. *J Nucl Med.* 2014;55:281–286.
21. Wu Z, Li ZB, Chen K, et al. microPET of tumor integrin $\alpha_v\beta_3$ expression using ^{18}F-labeled PEGylated tetrameric RGD peptide (^{18}F-FPRGD4). *J Nucl Med.* 2007;48:1536–1544.
22. Max R, Gerritsen RR, Nooijen PT, et al. Immunohistochemical analysis of integrin αvβ3 expression on tumor-associated vessels of human carcinomas. *Int J Cancer.* 1997;71:320–324.
23. Liu S. Radiolabeled cyclic RGD peptide bioconjugates as radiotracers targeting multiple integrins. *Bioconjug Chem.* 2015;26:1413–1438.
24. Tomasi G, Kenny L, Mauri F, Turkheimer F, Aboagye EO. Quantification of receptor-ligand binding with [^{18}F]fluciclatide in metastatic breast cancer patients. *Eur J Nucl Med Mol Imaging.* 2011;38:2186–2197.
25. Beer AJ, Grosu AL, Carlsen J, et al. [^{18}F]galacto-RGD positron emission tomography for imaging of αvβ3 expression on the neovasculature in patients with squamous cell carcinoma of the head and neck. *Clin Cancer Res.* 2007;13:6610–6616.
26. Kiessling LL, Pohl NL. Strength in numbers: non-natural polyvalent carbohydrate derivatives. *Chem Biol.* 1996;3:71–77.
27. Liu S. Radiolabeled cyclic RGD peptides as integrin $\alpha_v\beta_3$-targeted radiotracers: maximizing binding affinity via bivalency. *Bioconjug Chem.* 2009;20:2199–2213.
28. Wu Y, Zhang X, Xiong Z, et al. microPET imaging of glioma integrin $\alpha_v\beta_3$ expression using ^{64}Cu-labeled tetrameric RGD peptide. *J Nucl Med.* 2005;46:1707–1718.
29. Beer AJ, Lorenzen S, Metz S, et al. Comparison of integrin $\alpha_v\beta_3$ expression and glucose metabolism in primary and metastatic lesions in cancer patients: a PET study using ^{18}F-galacto-RGD and ^{18}F-FDG. *J Nucl Med.* 2008;49:22–29.
30. Zheng K, Liang N, Zhang J, et al. ^{68}Ga-NOTA-PRGD2 PET/CT for integrin imaging in patients with lung cancer. *J Nucl Med.* 2015;56:1823–1827.
31. Mi B, Yu C, Pan D, et al. Pilot prospective evaluation of ^{18}F-alfatide II for detection of skeletal metastases. *Theranostics.* 2015;5:1115–1121.
32. Chen SH, Wang HM, Lin CY, et al. RGD-K5 PET/CT in patients with advanced head and neck cancer treated with concurrent chemoradiotherapy: results from a pilot study. *Eur J Nucl Med Mol Imaging.* 2016;43:1621–1629.
33. Luan X, Huang Y, Gao S, et al. ^{18}F-alfatide PET/CT may predict short-term outcome of concurrent chemoradiotherapy in patients with advanced non-small cell lung cancer. *Eur J Nucl Med Mol Imaging.* 2016;43:2336–2342.
34. Zhang H, Liu N, Gao S, et al. Can an ^{18}F-ALF-NOTA-PRGD2 PET/CT scan predict treatment sensitivity to concurrent chemoradiotherapy in patients with newly diagnosed glioblastoma? *J Nucl Med.* 2016;57:524–529.